Frontiers in Bioscience Landmark

Front. Biosci. (Landmark Ed) **2022**; 27(4): 125
https://doi.org/10.31083/j.fbl2704125

Original Research

Anti-cancer Drug Anlotinib Promotes Autophagy and Apoptosis in Breast Cancer

Shuyi Chen[1,2,†], Yabiao Gao[2,†], Ping Zhu[1,2], Xue Wang[2,3], Linzi Zeng[2], Youping Jin[2], Xiuling Zhi[2], Huanjun Yang[1,4,5,*], Ping Zhou[2,*]

[1]Department of Radiation Oncology and Pathology, Fudan University Shanghai Cancer Center, Shanghai Medical College, Fudan University, 200032 Shanghai, China
[2]Department of Physiology and Pathophysiology, School of Basic Medical Sciences, Fudan University, 200032 Shanghai, China
[3]Department of Pathology, Ruijin Hospital, Shanghai Jiao Tong University School of Medicine, 200025 Shanghai, China
[4]Department of Oncology, Shanghai Medical College, Fudan University, 200032 Shanghai, China
[5]Shanghai Key Laboratory of Radiation Oncology, 200032 Shanghai, China
*Correspondence: zping@shmu.edu.cn (Ping Zhou); yanghj_1@hotmail.com (Huanjun Yang)
[†]These authors contributed equally.
Academic Editors: Nicholas Pavlidis and Stergios Boussios
Submitted: 23 February 2022 Revised: 19 March 2022 Accepted: 29 March 2022 Published: 7 April 2022

Abstract

Background: Anlotinib, a multi-target tyrosine kinase inhibitor, has significant anti-cancer effects on breast cancer (BC), lung cancer, colon cancer and ovarian cancer, but its mechanism has not been investigated in BC. **Methods**: The cell viability and growth of human non-triple negative BC cell line MCF-7 and triple negative BC cell line MDA-MB-231 with the treatment of anlotinib were tested by Cell Counting Kit-8 (CCK-8) assay and Ki67 staining. The alteration of genes related to apoptosis and autophagy were investigated by quantitative real-time reverse-transcription polymerase chain reaction (qRT-PCR), western blots and immunocytochemistry (ICC). Cell apoptosis was valued by TUNEL staining and flow cytometry. Further, mouse breast tumour cell lines AT-3 cells were subcutaneously injected into C57BL/6 mice, and the effect of anlotinib intragastrically on tumour growth *in vivo* was examined. **Results**: We found that anlotinib suppressed the cell viability and depressed Ki67 staining in MCF-7 and MDA-MB-231 cell lines. Besides, the drug also enhanced cell autophagy and apoptosis of MCF-7 and MDA-MB-231 cell lines, which could be rescued by autophagy inhibitors wortmannin (wort) and 3-methyladenine (3-MA), and BECN1 knockdown. Furthermore, Akt/GSK-3α pathway was inactivated by anlotinib treatment, while rescued by wort, 3-MA and silencing of BECN1 in the MCF-7 or MDA-MB-231 cells. We also found that anlotinib inhibited implanted tumour growth of BC in syngeneic mice. **Conclusions**: Our study demonstrated that anlotinib inhibited breast cancer cell growth *in vitro* and *in vivo*. Anlotinib promoted cell apoptosis and inactivated Akt/GSK-3α pathway of BC cells by inducing cell autophagy. It indicated that anlotinib may be an effective new drug for BC treatment.

Keywords: anlotinib; breast cancer; autophagy; apoptosis; proliferation

1. Introduction

Breast cancer (BC) is one of the most common and high-risk female malignant tumors worldwide. Its incidence rises each year, and the age of onset tends to be younger. At present, BC had surpassed lung cancer and became the most common cancer in the world, accounting for 11.7% of all new cancer cases in 2020 [1]. BC was also the most frequent cancer in female in 2020 in China and was estimated to be the fourth most common cancer diagnosed, replacing liver cancer [2]. Although the treatment of BC has improved in recent years, postoperative tumour cell recurrence, metastasis and drug resistance have resulted in short tumour-free survival and low 5-year survival rates in high-risk populations, which seriously threaten the lives and health of patients [2–4]. Targeted therapy, as a new therapeutic strategy, has the advantages of strong specificity, remarkable curative effects and few side effects. Hence, targeted therapy has been recognized as an effective and selective method to kill tumour cells, and it is gradually becoming a hot spot and trend in the field of cancer therapy.

Anlotinib hydrochloride, a novel oral multi-target tyrosine kinase receptor inhibitor that targets vascular endothelial growth factor receptor (VEGFR), fibroblast growth factor receptor (FGFR) and platelet-derived growth factor receptor (PDGFR), shows broad-spectrum inhibitory effects on tumour angiogenesis and growth [5,6]. *In vitro* studies have shown that anlotinib selectively inhibits VEGFR2/kinase insert domain receptor (KDR) and VEGFR3, with an inhibition rate 20 times that of sunitinib and 500 times that of sorafenib, respectively. In addition, the dysregulated FGF/FGFR axis promotes cancer progression and enhances the angiogenic potential of the tumour microenvironment, leading to an invasive phenotype of cancer cells [7–9], and FGF/FGFR signalling changes are associated with chemoresistance and adverse clinical prognosis of cancers. Part of reports shows that anlotinib inactivates FGFRs obviously, especially FGFR2,

compared with the effects of sorafenib in preclinical trials. Recently, it is found that anlotinib also inhibits c-Kit receptor, glial cell-derived neurotrophic factor receptor tyrosine kinase, Aurora-B kinase, c-Fms kinase and discoid domain receptor 1, which are involved in the cell proliferation of colon cancer, lymphoma, and acute T cell leukaemia or in the progression of lung, breast, and ovarian cancers [10–13]. *In vivo* experiments also demonstrates that anlotinib has broad inhibitory effects against xenograft tumors from transplanted human colon, ovarian, kidney and lung cancer cells and glioma cells [14].

It has been shown that anlotinib has anti-cancer effects on many malignant tumors remarkably, such as non-small cell lung cancer, renal cell carcinoma and hepatocellular carcinoma in clinical trials. Recently, the clinical trials of triple-negative BC and metastatic HER2-negative BC have been carried out, however, there is still a lack of in-depth research on the role of anlotinib in BC and its underlying mechanism. Especially, BC can be divided into three main sub-types at least, including triple negative BC, HER2 Enriched BC and Luminal (A and B) BC. Hence, in this study, we used triple negative BC cell line MDA-MB-231 and non-triple negative, luminal, BC cell line MCF-7 to explore the effects of anlotinib on the growth of different types of BC and its underlying mechanism, which provided a new choice for targeted therapy of BC.

2. Materials and Methods

2.1 Compounds and Antibodys

Anlotinib was kindly given as a gift by Chia Tai Tianqing Co., Ltd. (Nanjing, JS, China). Wortmannin (Wort) and 3-methyladenine (3-MA) were purchased from APExBIO (Houston, TX, USA). The antibodies for western blotting, immunocytochemistry and immunohistochemistry were listed in the **Supplementary Table 1**.

2.2 Cell Culture and Transfection

The human BC cell lines MCF-7 and MDA-MB-231 were purchased from the cell bank of the Chinese Academy of Science. MCF-7 was cultured in Dulbecco's modified Eagle's medium (DMEM) containing 10% foetal bovine serum (FBS) and antibiotics (penicillin 100 U/mL and streptomycin 100 mg/mL) in a 37 °C humidified atmosphere with 5% CO_2. MDA-MB-231 was cultured in Leibovitz's L-15 medium with 10% FBS and antibiotics at 37 °C in a free gas exchange environment with atmospheric air. The mouse breast carcinoma cell line AT3 were obtained from Roswell Park Cancer Institute (Buffalo, NY, USA) [15], and were cultured in Roswell Park Memorial Institute (RPMI) 1640 medium with 10% FBS and antibiotics in a 37 °C humidified atmosphere with 5% CO_2.

For silencing of BECN1, siRNAs were transiently transfected into cells using jetPRIME® transfection reagent according to the manufacturer's instructions (Polyplus transfection®SA, France).

2.3 Cell Viability Assay

A Cell Counting Kit-8 (CCK-8) assay was used to detect cell viability. Briefly, 10000 cells for MCF-7 cell and 5000 cells for MDA-MB-231 cell per well were seeded in 96-well plates and incubated with anlotinib at various concentrations and for different time points. The CCK-8 reagent was then added at a 1:10 dilution and incubated for 1.5 h, and the absorbance at 450 nm was measured on a microplate reader to calculate the cell viability and IC50.

2.4 Quantitative Real-time PCR (qRT-PCR)

RNA was extracted from the cells or tissues using the TRIzol-trichloromethane-isopropanol method and reverse transcribed into cDNA using ReverTra Ace qPCR RT Kit (TOYOBO CO., LTD., Osaka, Japan). The mixtures contained samples of 10 ng (1 μL), SYBR Green of 5 μL, and primers of 2 μL. The sequences of the primers are listed in **Supplementary Table 2**.

2.5 Western Blot Analysis

Protein samples from cancer cells and tissues were resolved by SDS-PAGE (10% or 12%), electrotransferred onto Immobilon-P membranes, blocked, and incubated with primary and secondary antibodies. Densitometric quantification of the protein bands was analysed using ImageJ 1.8.0 software (National Institutes of Health, Bethesda, MD, USA).

2.6 Flow Cytometry

For apoptosis analysis, MCF-7 and MDA-MB-231 cells were collected and stained using Annexin V-FITC/PI apoptosis detection kit (Vazyme, Nanjing, JS, China). The samples were tested on a flow cytometer (FACSCalibur) and analysed by ModFit LT v.3.0 software (Verity Software House, Topsham, ME, USA).

2.7 Immunocytochemistry (ICC) and TUNEL Staining Assays

Cells were fixed in 4% paraformaldehyde (PFA) for 15 min and then permeabilized with 0.1% Triton X-100 for 20 min. After blocking with 5% goat serum for 2 h, the cells were incubated with primary antibodies against Ki67, BECN1 and LC3B overnight at 4 °C. Then, the cells were washed and incubated with secondary antibodies and finally incubated with DAPI for nuclei staining. Images were taken with an Olympus microscope (OLYMPUS, Tokyo, Japan). For the TUNEL staining assay, cells were fixed with 4% PFA first and then stained using TUNEL BrightRed Apoptosis Detection Kit (Vazyme, Nanjing, JS, China).

2.8 Immunohistochemistry

Dissected tumour tissues were preserved in 4% PFA at 4 °C for 24 h, dehydrated with xylenes and alcohols, and embedded in paraffin. Sections were cut at a thickness of 5 μm, dewaxed in xylene, rehydrated through decreasing

concentrations of ethanol, and washed in PBS. Antigens were unmasked, blocked, and incubated with primary antibodies overnight at 4 °C. Then sections were incubated with secondary antibodies and DAPI. Images were taken with an Olympus microscope.

2.9 Syngeneic Mouse Model

Sixteen male wild-type C57BL/6 mice were purchased from the Laboratory Animal Resources of Chinese Academy of Sciences (Shanghai, China). Mice were maintained in specific pathogen free (SPF) conditions at the Fudan University Animal Experimental Centre, compliant with the guidelines of the National Institutes of Health Guide for the Care and Use of Laboratory Animals. The experiment was approved by the Institutional Animal Care and Utilization Committee of Fudan University (Approval number: 20190703). AT-3 cells were harvested and resuspended at 1×10^7 cell/mL, and the 0.1 mL of suspension was subcutaneously injected into the 16 male mice. On day 7 after injection, 10 mice randomly were administered 2.5 mg/kg anlotinib intragastrically once daily for 3 weeks (anlotinib group, n = 10), while other 6 mice were treated with the same volume of 0.25% DMSO (DMSO group, n = 6). The mice were sacrificed after 4 weeks of cell injection, and the tumors were removed and measured.

2.10 Statistical Analysis

Statistical analysis was performed by Student's *t*-test for comparisons between the DMSO and anlotinib groups and two-factor Analysis of Variance (ANOVA) for comparisons among the four groups, followed by a subsequent post-hoc test. Growth curves descripted in the CCK-8 assay were analysed with two-factor ANOVA (Treatment $\times$ time). The experiments were repeated at least 3 times independently. The data were presented as mean $\pm$ SD and analysed using GraphPad Prism 8.0.1 (GraphPad, San Diego, CA, USA), and $p < 0.05$ was considered statistically significant.

3. Results

3.1 Anlotinib Suppressed the Cell Viability and Proliferation of MCF-7 and MDA-MB-231 Cells

The CCK-8 assay was used to assess cell viability and the half maximal inhibitory concentration (IC50) in MCF-7 and MDA-MB-231 cells. The results showed that anlotinib inhibited cell viability in a dose- and time-dependent manner. The IC50 values of MCF-7 cells treated with anlotinib for 4 h, 12 h, 24 h and 48 h were 34.02 $\pm$ 0.026 μM, 26.08 $\pm$ 0.030 μM, 17.38 $\pm$ 0.018 μM and 12.06 $\pm$ 0.038 μM, respectively (Fig. 1A). And IC50 values of MDA-MB-231 were 42.57 $\pm$ 0.029 μM, 32.06 $\pm$ 0.026 μM, 27.72 $\pm$ 0.031 μM and 16.27 $\pm$ 0.036 μM after anlotinib treated for 4 h, 12 h, 24 h and 48 h (Fig. 1B). The IC50 value of anlotinib in MCF-7 is smaller than that in MDA-MB-231 in a time-dependent manner, indicating that MCF-7 is more sensitive to anlotinib. We also performed Ki67 staining, and the results showed that number of positive staining of MCF-7 and MDA-MB-231 cells was decreased with anlotinib administration (Fig. 1C–D, n = 6, $^{**}p < 0.01$ vs DMSO). Therefore, anlotinib suppressed the proliferation of MCF-7 and MDA-MB-231 cells.

3.2 Anlotinib Induced Apoptosis in MCF-7 and MDA-MB-231 Cells

We next explored the apoptosis of MCF-7 and MDA-MB-231 cells with anlotinib treatment. The results revealed that both early and late apoptosis in MCF-7 and MDA-MB-231 cells were increased significantly after anlotinib treatment (Fig. 2A, $^{*}p < 0.05$, $^{**}p < 0.01$, n = 3). The apoptosis induction analysis revealed that a larger proportion of early and late apoptosis was counted in the MCF-7 cells compared with MDA-MB-231 cells. Consistently, TUNEL staining also showed that number of positive staining (red) cells was increased after anlotinib treatment (Fig. 2B and 2C, n = 6, $^{**}p < 0.01$ vs DMSO). Furthermore, anlotinib upregulated the mRNA levels of proapoptotic genes, including BAX, BAD, BID, Caspase1, Caspase3, Caspase8 and Caspase9, and the protein levels of Bak, Cytochrome C, cleaved Caspase1, cleaved Caspase3, cleaved PARP1 and cleaved Caspase9 in MCF-7 and MDA-MB-231 cells (Fig. 3D, E and F, $^{*}p < 0.05$, $^{**}p < 0.01$, n = 3). Moreover, the mRNA and protein levels of the anti-apoptotic gene Bcl-2 were downregulated after anlotinib treatment (Fig. 3D, E and F, $^{*}p < 0.05$, $^{**}p < 0.01$, n = 3). The results indicated that anlotinib promoted apoptosis in MCF-7 and MDA-MB-231 cells.

3.3 Anlotinib Promoted Autophagy in Human BC MCF-7 and MDA-MB-231 Cells

Cell autophagy is associated with cell proliferation and apoptosis. Then, we detected the expression of autophagy-related markers in MCF-7 and MDA-MB-231 cells with anlotinib induction. We found that anlotinib upregulated LC3B, BECN1and ATG4B mRNA levels in MCF-7 cells (Fig. 3A, $^{*}p < 0.05$, n = 3), while upregulated LC3B, BECN1and ATG7 mRNA levels in MDA-MB-231 cells (Fig. 3B, $^{*}p < 0.05$, n = 3). At protein level, anlotinib also increased the ratio of LC3BII to LC3BI and BECN1, while decreased p62 (Fig. 3C, D and E, $^{*}p < 0.05$, $^{**}p < 0.01$, n = 3) in MCF-7 and MDA-MB-231 cells. Moreover, both numbers of BECN1 (green) and LC3B (red) positive staining cells were increased after anlotinib treatment (Fig. 3F and G, H; n = 6, $^{**}p < 0.01$ vs DMSO). The results indicated that anlotinib induced autophagy in MCF-7 and MDA-MB-231 cells.

3.4 Anlotinib Induced Apoptosis by Promoting Autophagy in MCF-7 and MDA-MB-231 Cells

Autophagy is a double-edged sword in tumour progression and therapy and is closely related with apoptosis

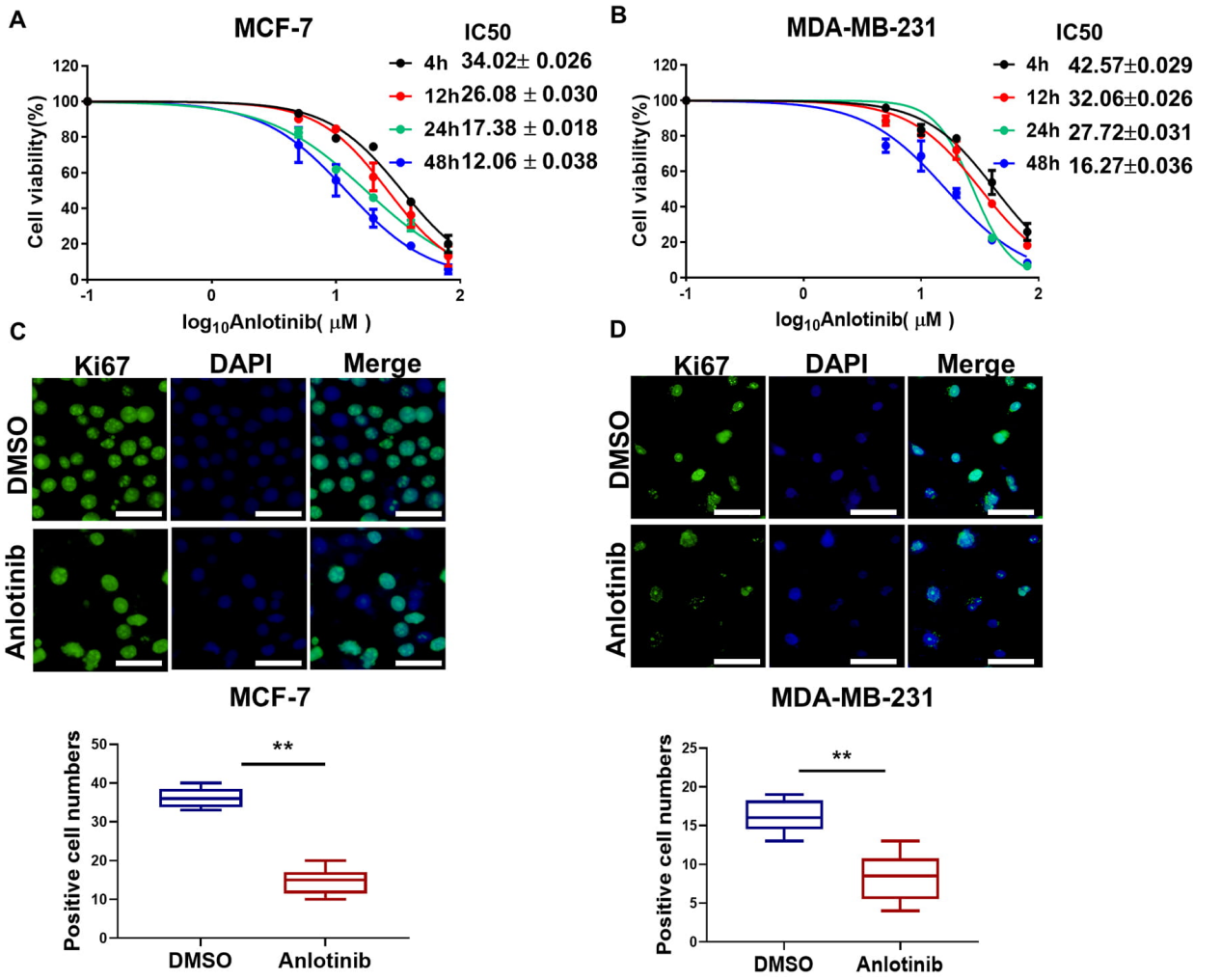

Fig. 1. Anlotinib suppressed the proliferation of human BC cells. (A and B) Dose-response curves of anlotinib treatment. Cells were cultured with anlotinib at various concentrations for 4, 12, 24 and 48 h, and cell viability was detected by CCK-8 assay. (C and D) Representative images of Ki67 staining. The MCF-7 and MDA-MB-231 cells were stained after anlotinib treatment with 10 μM for 12 h. Scale bars: 50 μm. The data are shown as the mean $\pm$ SD. $^{*}p < 0.05$, $^{**}p < 0.01$ vs DMSO, n = 6.

in cancer cell growth. To confirm the role of autophagy in anlotinib-induced apoptosis, MCF-7 and MDA-MB-231 cells were pre-treated with the autophagy inhibitors wortmannin (wort, 1 μM) and 3-methyladenine (3-MA, 20 μM) before anlotinib (10 μM) treatment. The ratio of protein LC3BII to LC3BI was decreased in autophagy inhibitors pre-treated and BECN1 knockdown cells compared to those only treated with anlotininb, while the protein level of p62 was increased (Fig. 4A–D and **Supplementary Fig. 1A,B**, $^{**}p < 0.01$ vs DMSO, $^{\#}p < 0.05$, $^{\#\#}p < 0.01$ vs Anlotinib, n = 3). Wort and 3-MA pre-treated, and loss of BECN1 rescued the protein level of the apoptotic markers cleaved PARP1 and Bak in MCF-7 and MDA-MB-231 cells with anlotinib treatment (Fig. 4A–D, **Supplementary Fig. 1A,B**, $^{*}p < 0.05$, $^{**}p < 0.01$ vs DMSO, $^{\#}p < 0.05$, $^{\#\#}p < 0.01$ vs Anlotinib, n = 3). These data suggested that anlotinib at least partly, if not entirely, induced apoptosis by promoting autophagy in MCF-7 and MDA-MB-231 cells.

3.5 Anlotinib Regulated the Akt/GSK-3α Pathway Through Cell Autophagy

Given that anlotinib showed significant therapeutic efficacy in BC cells, we further determined the underlying mechanism. Recent report revealed that the level of Akt (S473) and GSK-3α/β(S21/S9) phosphorylation was positively correlated with the level of apoptosis and autophagy [16]. Our results showed that anlotinib decreased the phosphorylation of Akt and GSK-3α but had no effect on the protein levels of total Akt or GSK-3α in MCF-7 and MDA-MB-231 cells (Fig. 5A–D, **Supplementary Fig. 1C**, $^{*}p < 0.05$, $^{**}p < 0.01$ vs DMSO, n = 3). Wort and 3-MA pre-treatment, and loss of BECN1 increased Akt and GSK-3α phosphorylation with anlotinib treatment (Fig. 5A–D, **Supplementary Fig. 1C**, $^{\#}p < 0.05$, $^{\#\#}p < 0.01$ vs anlotinib, n = 3). These findings indicated that anlotinib suppressed Akt activation and enhanced GSK-3α activation through autophagy induction in MCF-7 and MDA-MB-231 cells.

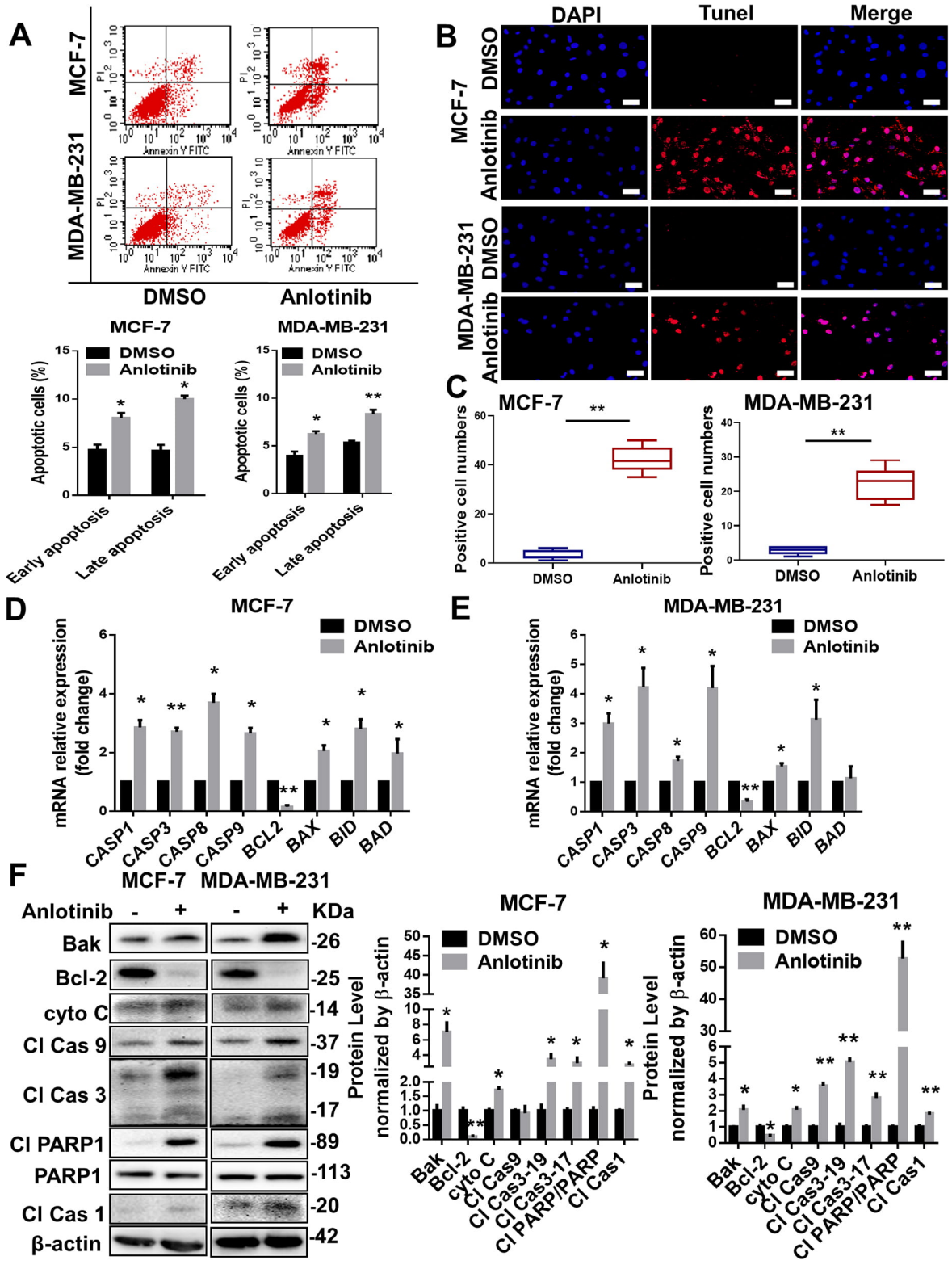

Fig. 2. Anlotinib promoted apoptosis in human BC cells. The MCF-7 and MDA-MB-231 cells were induced by anlotinib with 10 μM for 24 h. (A) The ratio of early and late apoptotic cells was measured in MCF-7 and MDA-MB-231 cells treated with DMSO or anlotinib. Apoptosis was detected by Annexin V-FITC and propidium iodide (PI) staining. (B and C) The apoptotic level in the anlotinib-treated cells was detected by TUNEL staining. Scale bars: 25 μm. (D and E) The mRNA level of apoptotic-associated molecules was increased markedly in anlotinib-treated cells. (F) Western blot showing the expression of apoptosis-associated proteins (left). Quantitative summary of the blots in the right panel; the data were normalized to β-actin. The data are shown as the mean $\pm$ SD. $^{*}p < 0.05$, $^{**}p < 0.01$ vs DMSO, n = 3.

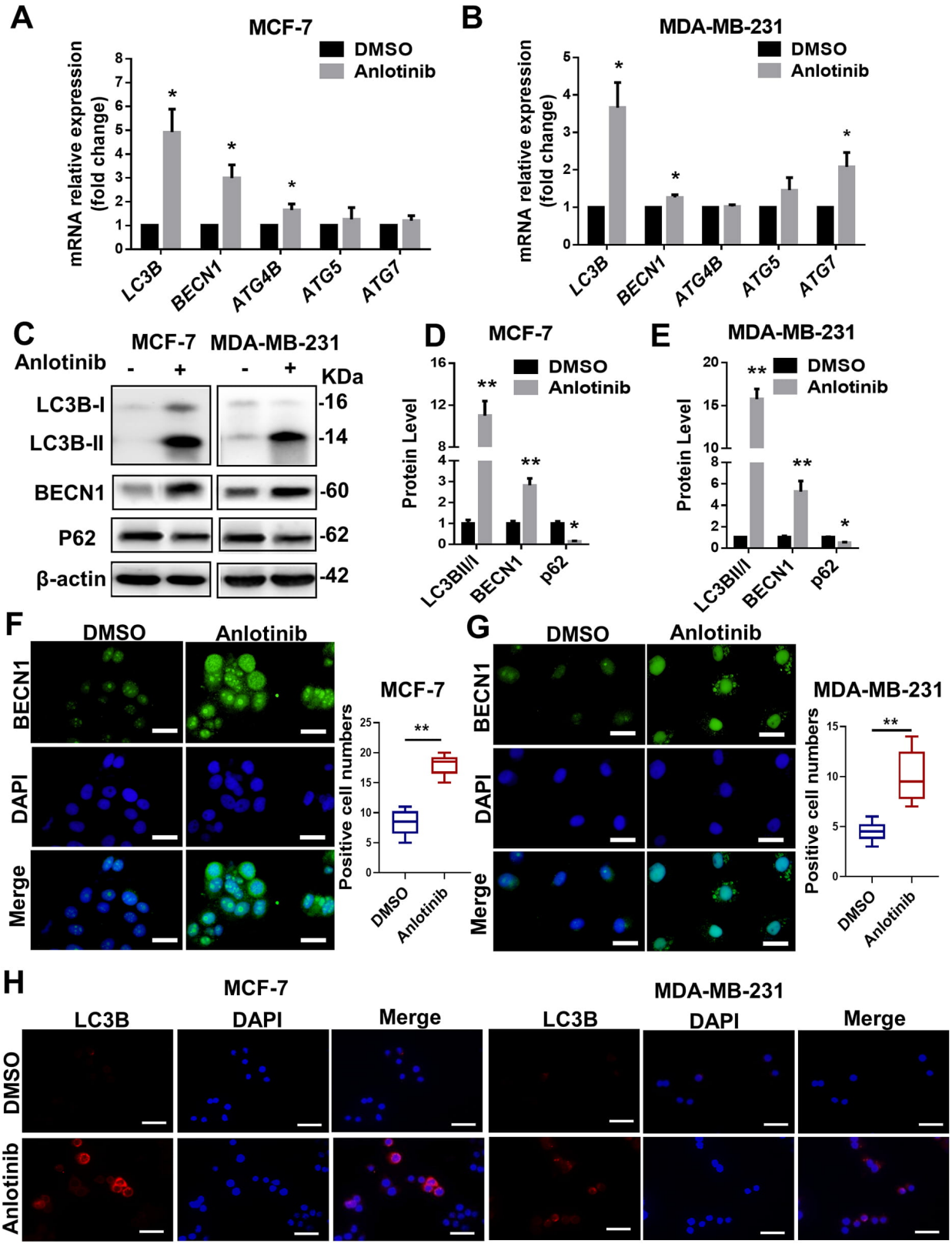

Fig. 3. Anlotinib induced autophagy with 10 μM for 24 h in human BC cell lines. (A and B) The mRNA level of autophagy-related molecules was increased markedly in anlotinib-treated cells. (C) Western blot showing the expression of autophagy-related proteins. (D and E) Quantitative summary of the blots in panel C for autophagy-related proteins; the data were normalized to β-actin. (F and G) Representative images of BECN1 staining. The data are shown as the mean $\pm$ SD. $^{*}p < 0.05$, $^{**}p < 0.01$ vs DMSO, n = 3. (H) Representative images of LC3B staining. Scale bars: 100 μm.

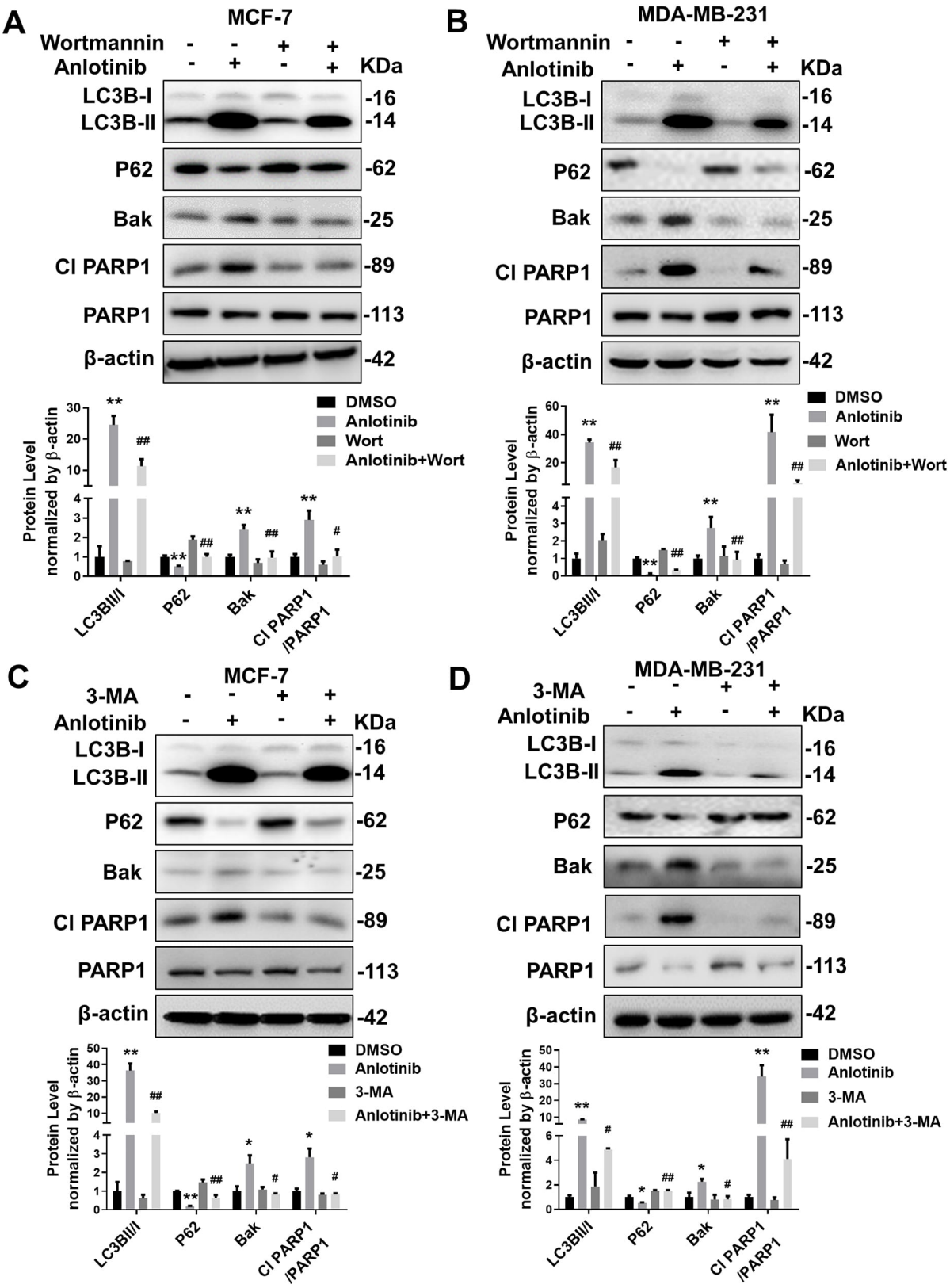

Fig. 4. Anlotinib induced apoptosis by promoting autophagy in MCF-7 and MDA-MB-231 cells with the mount of 10 μM for 24 h. (A and B) The autophagy inhibitor wort protected BC cells from anlotinib-induced apoptosis. (C and D) The autophagy inhibitor 3-MA protected BC cells from anlotinib-induced apoptosis. Western blot showing the ratio of LC3B II/LC3B I and the expression of p62 and apoptosis-associated proteins and the analysis. The data are shown as the mean ± SD. $^{*}p < 0.05$, $^{**}p < 0.01$ vs DMSO, $^{\#}p < 0.05$, $^{\#\#}p < 0.01$ vs Anlotinib, n = 3.

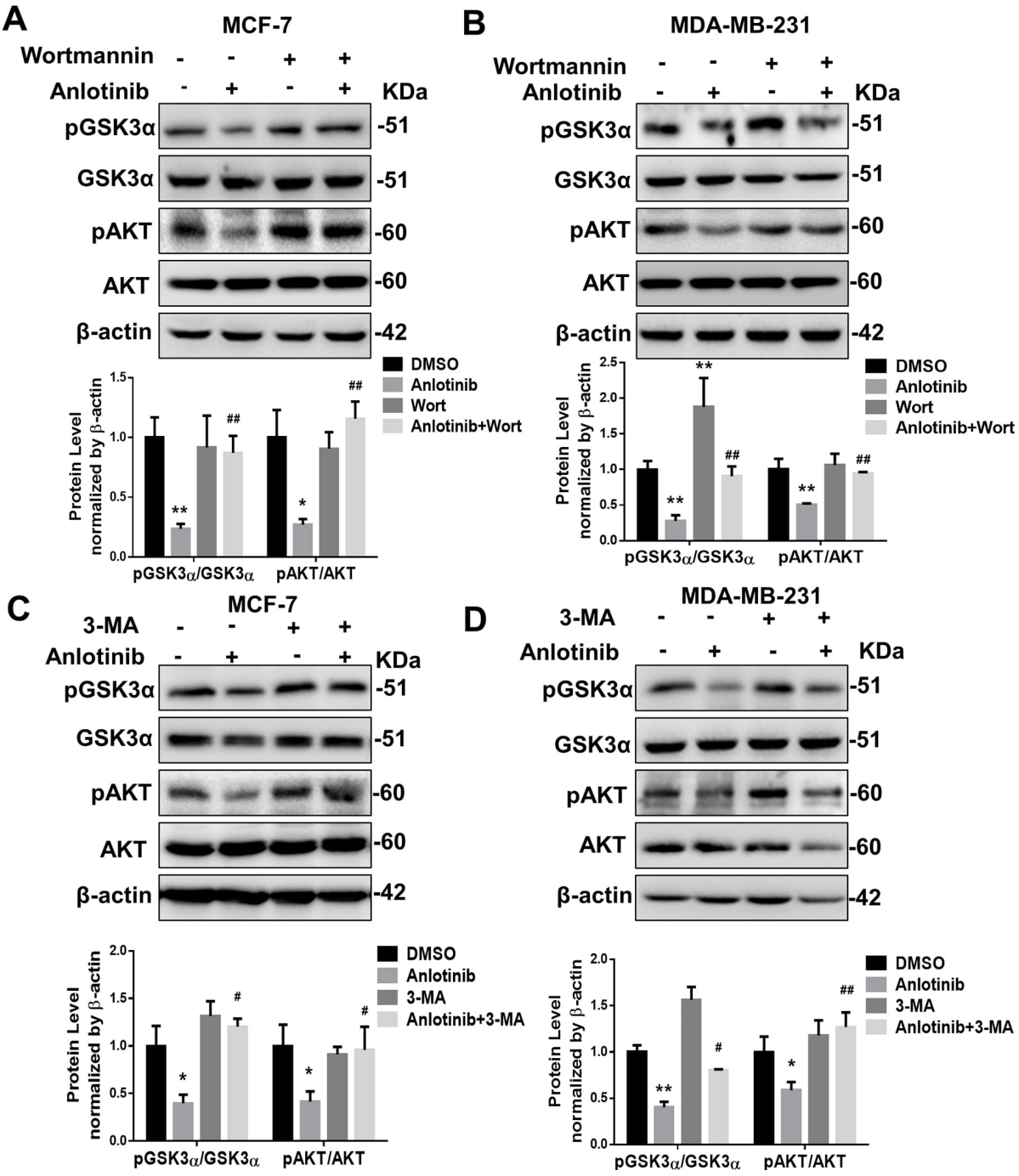

Fig. 5. Anlotinib regulated the Akt/GSK-3α pathway through cell autophagy. (A–D) MCF-7 and MDA-MB-231 cells were pretreated with the autophagy inhibitors wort (1 μM) and 3-MA (20 μM) before anlotinib (10 μM) treatment in 24 hrs. The four groups were analysed by western blotting with total and phosphorylated antibodies for Akt and GSK-3α, and the data were normalized to β-actin. The data are shown as the mean $\pm$ SD. $^{*}p < 0.05$, $^{**}p < 0.01$ vs DMSO, $^{\#}p < 0.05$, $^{\#\#}p < 0.01$ vs Anlotinib, n = 3.

3.6 Anlotinib Suppressed BC Growth in vivo

To examine the therapeutic significance *in vivo*, mice were subcutaneously injected with AT-3 cells to generate syngeneic tumors followed by continuous 3-week intragastric treatment with anlotinib. The anlotinib group mice showed significantly decreased body weight, tumour weight and tumour volume compared to those of the DMSO group. The body weight of mice fed with anlotinib was not significantly different from that of mice without anlotinib in the first two weeks. However, the weight of mice treated with anlotinib was increased significantly during the last two weeks. The result comprehensively demonstrated that anlotinib inhibited tumour growth (Fig. 6A–D, $^{*}p <$ 0.05 vs DMSO, DMSO group n = 6, anlotinib group n =

10). Consistent with the cell-based assay, the mRNA levels of LC3B, ATG4B and ATG5 in tumour from the anlotinib group were upregulated (Fig. 6E, $^{**}p < 0.01$ vs DMSO), and the ratio of LC3BII to LC3BI protein also increased, suggesting that anlotinib induced autophagy of BC *in vivo*. The proapoptotic protein cleaved caspase-3 was expressed at higher levels in the tumour from the anlotinib group than in the DMSO group, and the anti-apoptotic protein Bcl-2 showed the opposite result. These results indicated that induction of apoptosis occurred in anlotinib-treated syngeneics (Fig. 6F–G, $^{*}p < 0.05$, $^{**}p < 0.01$ vs DMSO, DMSO = 6, anlotinib = 8). Anlotinib group mice had fewer Ki67-positive cells compared to those of DMSO group mice, indicating that the number of proliferating cells was reduced (Fig. 6H, $^{*}p < 0.05$, $^{**}p < 0.01$, DMSO = 6, anlotinib = 8). These data demonstrated that anlotinib inhibited BC growth *in vivo*.

4. Discussion

Anlotinib, an inhibitor of multiple tyrosine kinase receptors, inhibits tumour progression by inhibiting angiogenesis [17], but there is no published literature on the inhibitory mechanism of anlotinib on BC.

Many studies have reported that anlotinib exerts antitumour effects to inhibit cell viability and proliferation in hepatocellular carcinoma (HCC), lung cancer, thyroid cancer, and osteosarcoma [16,18–20]. Our study found that anlotinib also inhibited the cell viability and proliferation of BC cells, which was consistent with the effects in other tumors.

Autophagy is an important cellular mechanism that plays a "housekeeping" role in normal physiological processes, including the removal of longevity, aggregation and misfolded proteins, removal of damaged organelles, and the regulation of growth and ageing. In tumour cells, autophagy is usually activated during anticancer treatments such as radiation therapy, chemotherapy, and targeted therapy. This may be a cytoprotective mechanism that also causes excessive autophagy in the cell, namely, excessive self-digestion, and induces phagocytic cell death, which is also known as type II programmed cell death [21]. A study found that anlotinib induced autophagy in human lung cancer cells in a time- and concentration-dependent manner and increased the ratio of LC3BII/I protein and the protein expression level of BECN1. The autophagy inhibitors 3-MA and small interfering RNA of BECN1 reversed the autophagy effect induced by anlotinib, unexpectedly, they both enhanced the inhibitory effect of anlotinib on cell proliferation, making the anticancer effect of anlotinib more sensitive and strengthening its inhibition of angiogenesis [19]. These findings suggested that the induction of autophagy in human lung cancer cells by anlotinib is a cytoprotective effect. In our study, anlotinib also induced autophagy in MCF-7 and MDA-MB-231 human BC cells. These results showed significantly increased mRNA and protein expression levels of LC3B and BECN1 and the ratio of protein LC3BII/I and BECN1 levels and decreased P62 levels, suggesting that anlotinib promotes autophagic cell death in BC cells.

Apoptosis is a common programmed cell death and plays a key role in the development of diseases, including cancer. Cancer cells evade apoptosis, thereby achieving excessive proliferation and surviving under hypoxic conditions and with drug resistance [22]; thus, promoting tumour cell apoptosis has become an important strategy for the treatment of cancer. Studies have shown that anlotinib exerts its antitumour effects on HCC, thyroid cancer, osteosarcoma, and lung cancer by promoting apoptosis [16,18–20,23]. Anlotinib significantly inhibited colony formation and promoted apoptosis in HCC and thyroid cancer *in vitro* [16,18]. It upregulated the pro-apoptotic molecule Bax and inhibited the anti-apoptotic proteins Bcl-2 and Survivin to kill tumour cells. In addition, animal experiments demonstrated that anlotinib reduced the volumes and weights of transplanted tumors [18]. In thyroid cancer, anlotinib caused abnormal spindle assembly and G2/M arrest, promoted the activation of cleaved-Caspase 3 and cleaved PARP, and activated TP53 [16]. Like the above experimental results, we found that anlotinib increased the mRNA and protein levels of proapoptotic proteins and inhibited the mRNA and protein levels of the anti-apoptotic protein Bcl-2 in MCF-7 and MDA-MB-231 BC cells, thereby exerting an antitumour effect.

Autophagy and apoptosis often occur in the same cells with the same upstream cellular signals activated by the endoplasmic reticulum, such as extracellular regulated protein kinases (ERK)/activating transcription factor 4 (ATF4), Inositol-requiring enzyme-1α, ATF6, and Ca^{2+}. Autophagy blocks the induction of apoptosis by inhibiting the activation of apoptosis-associated caspases or by reducing cell damage. Meanwhile, activation of apoptosis-related proteins also suppresses autophagy by degrading autophagy-related proteins such as BECN1, autophagy-related protein 4D (ATG4D), ATG3 and ATG5, but the specific mechanisms between the interaction in BC cells need further study [24]. However, in our study, we utilized the autophagy inhibitors wort and 3-MA before anlotinib treatment and found that inhibition of autophagy reversed anlotinib-induced apoptosis in BC cells. The similarity results also have been found in the MDA-MB-231 cells transfected with BECN1 siRNA, indicating that loss of BECN1 recued anlotinib-induced apoptosis. We obtained the opposite results compared with that reported in lung cancer cells [19]. This is probably due to the different concentrations of autophagy inhibitors and different cells, but it remains unclear and needs further study to clarify the crosstalk between apoptosis and autophagy.

Our study indicates that anlotinib has both effects on triple negative breast cancer cells and non-triple negative breast cancer cells. The IC50 value of anlotinib in MCF-7

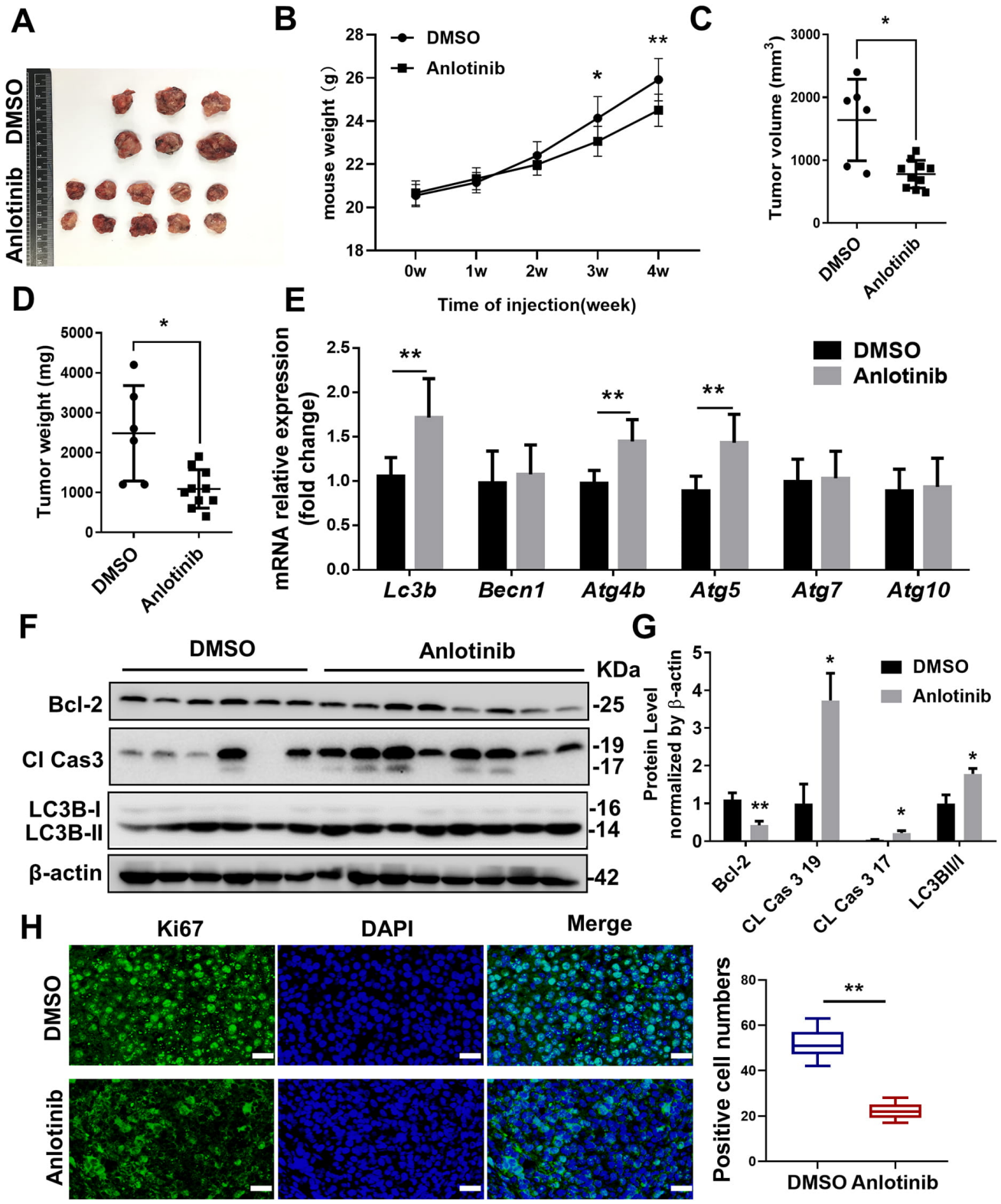

Fig. 6. Anlotinib suppressed BC growth *in vivo*. (A) Images of dissected tumors from C57BL/6 mice injected with AT-3 cells in the DMSO-treated group (n = 6) and the anlotinib-treated group (n = 10). (B) The body weight of the mice after injection over time. (C) Tumour volumes were decreased in the anlotinib group compared to those of the DMSO group. (D) Tumour weights with anlotinib treatment were heavier than those without anlotinib treatment. (E) The mRNA level of autophagy-associated molecules was increased markedly in the anlotinib-treated tumour tissues. (F and G) The ratio of LC3B II/LC3B I and the expression level of Bcl-2 and Cl-Caspase 3 were detected by western blotting and analysis. (H) Ki67 immunohistochemistry staining of tumour sections from DMSO and anlotinib mice. Scale bars: 50 μm. The data are shown as the mean ± SD. $^{*}p < 0.05$, $^{**}p < 0.01$ vs DMSO.

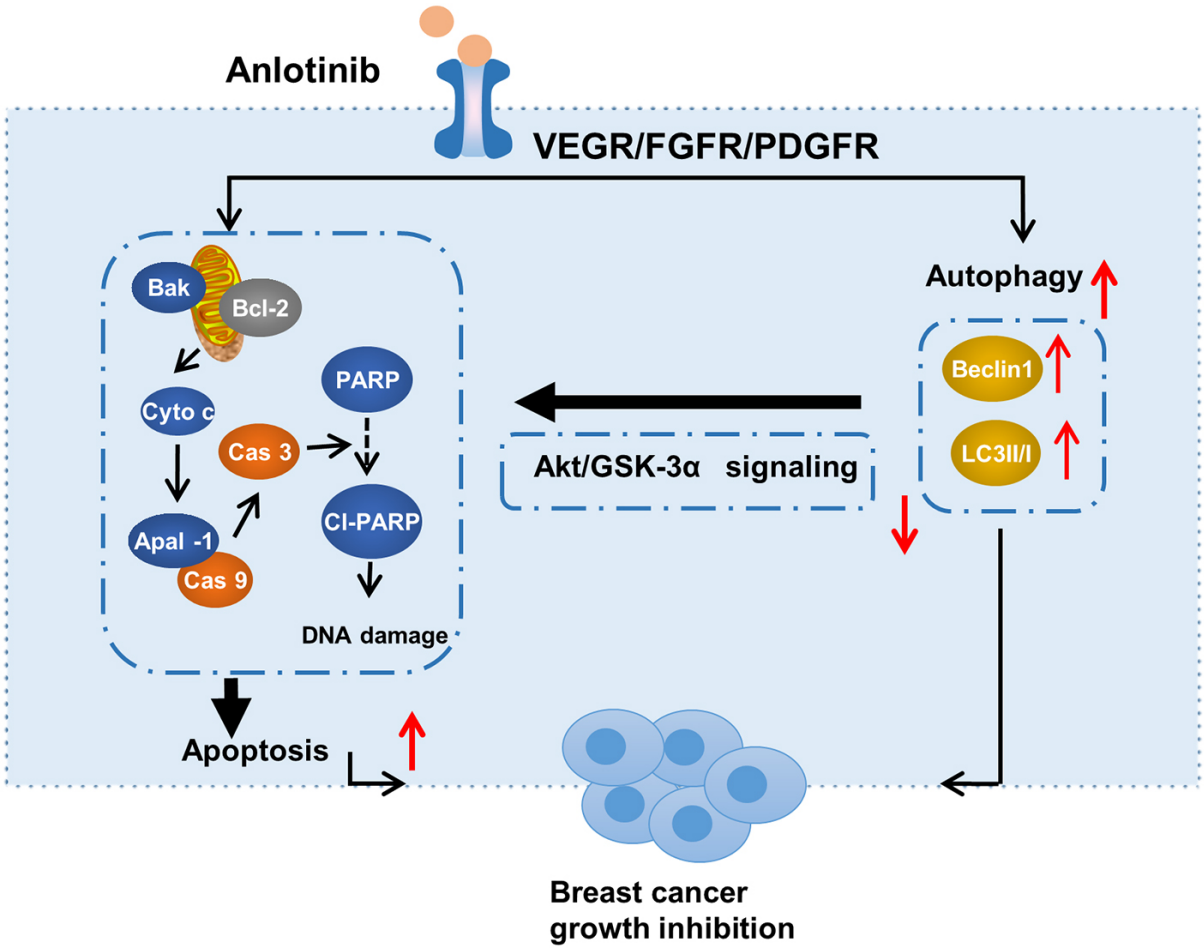

Fig. 7. The mechanism by which anlotinib exerted its anticancer effect in BC.

is smaller than that in MDA-MB-231 in a time-dependent manner, demonstrating that anlotinib has a stronger effect to kill neoplasm cells in non-triple negative breast cancer. The apoptosis induction analysis revealed that a larger proportion of early and late apoptosis was counted in the MCF-7 cells compared with MDA-MB-231 cells. These results may reveal that anlotinib is more effective in the treatment of non-triple negative breast cancer.

Evidence indicates that Akt is a key molecule in both autophagy and apoptosis because it is the upstream signal of mammalian target of rapamycin complex and JNK [25–27]. Previous studies reported that anlotinib inhibits Erk and Akt signal transduction pathways to regulate cell growth in HCC cells [18]. Akt/GSK-3 signals can regulate cell autophagy, apoptosis, and cell cycle. Furthermore, level of Akt (S473) and GSK-3α/β(S21/S9) phosphorylation was positive correlated with the level of apoptosis and autophagy in a lung adenocarcinoma cell line [28]. Hence, we investigated Akt signalling and found that inactivated Akt/GSK-3α signalling in anlotinib-induced cells was reversed by autophagy inhibitors and BECN1 deficiencies, suggesting that anlotinib-induced autophagy regulated Akt/GSK-3α signalling (Fig. 7). We conjecture that autophagy and Akt might regulate each other, forming a closed circuit.

5. Conclusions

In summary, our study demonstrated that anlotinib inhibited the growth of BC *in vitro* and *in vivo*, especially in non-triple negative, luminal, BC cell line MCF-7 cells. Anlotinib promoted cell apoptosis and inactivated Akt/GSK-3α pathway of BC cells, by autophagy induction. Therefore, anlotinib may be an effective new drug for BC treatment.

Abbreviations

3-MA, 3-methyladenine; ATF4, activating transcription factor 4; ATG, autophagy-related protein; BC, Breast cancer; ERK, extracellular regulated protein kinases; FGFR, fibroblast growth factor receptor; PFA, paraformaldehyde; PDGFR, platelet-derived growth factor receptor; VEGFR, vascular endothelial growth factor receptor; wort, wortmannin.

Author Contributions

PZ (Ping Zhou) and HY conceived the idea and designed the research study. SC designed and performed most experiments, analyzed the data, and wrote the manuscript. YG repeated some experiments. PZ (Ping Zhu) and YJ provided help and advice on animal experiment. XW and LZ analyzed the data. XZ provided advice on the study and manuscript.

Ethics Approval and Consent to Participate

All animal care and experimental procedures complied with the guidelines of the National Institutes of Health Guide for the Care and Use of Laboratory Animals. The experiment was approved by the Institutional Animal Care and Utilization Committee of Fudan University (Approval number: 20190703).

Acknowledgment

Thanks to all the peer reviewers for their opinions and suggestions.

Funding

This study was supported by Medical Science Research Foundation from Beijing Medical and Health Foundation (F2190E), and Medical Science Research Foundation from Bethune Charitable Foundation (B19358ET).

Conflict of Interest

The authors declare no conflict of interest.

Supplementary Material

Supplementary material associated with this article can be found, in the online version, at https://doi.org/10.31083/j.fbl2704125.

References

[1] Sung H, Ferlay J, Siegel RL, Laversanne M, Soerjomataram I, Jemal A, *et al*. Global Cancer Statistics 2020: GLOBOCAN Estimates of Incidence and Mortality Worldwide for 36 Cancers in 185 Countries. CA: A Cancer Journal for Clinicians. 2021; 71: 209–249.

[2] Cao W, Chen H, Yu Y, Li N, Chen W. Changing profiles of cancer burden worldwide and in China: a secondary analysis of the global cancer statistics 2020. Chinese Medical Journal. 2021; 134: 783–791.

[3] Li L, Gao Q, Xu G, Shi B, Ma X, Liu H, *et al*. Postoperative recurrence analysis of breast cancer patients based on clinical serum markers using discriminant methods. Cancer Biomarkers. 2017; 19: 403–409.

[4] Ma R, Feng Y, Lin S, Chen J, Lin H, Liang X, *et al*. Mechanisms involved in breast cancer liver metastasis. Journal of Translational Medicine. 2015; 13: 64.

[5] Zhong C, Chen F, Yang J, Jia W, Li L, Cheng C, *et al*. Pharmacokinetics and disposition of anlotinib, an oral tyrosine kinase inhibitor, in experimental animal species. Acta Pharmacologica Sinica. 2018; 39: 1048–1063.

[6] Lin B, Song X, Yang D, Bai D, Yao Y, Lu N. Anlotinib inhibits angiogenesis via suppressing the activation of VEGFR2, PDGFRβ and FGFR1. Gene. 2018; 654: 77–86.

[7] Wesche J, Haglund K, Haugsten E. Fibroblast growth factors and their receptors in cancer. Biochemical Journal. 2011; 437: 199–213.

[8] Turner N, Grose R. Fibroblast growth factor signalling: from development to cancer. Nature Reviews Cancer. 2010; 10: 116–129.

[9] Knights V, Cook SJ. De-regulated FGF receptors as therapeutic targets in cancer. Pharmacology & Therapeutics. 2010; 125: 105–117.

[10] Kakiuchi-Kiyota S, Lappin PB, Heintz C, Brown PW, Pinho FO, Ryan AM, *et al*. Expression of proto-oncogene cFMS protein in lung, breast, and ovarian cancers. Applied Immunohistochemistry & Molecular Morphology. 2014; 22: 188–199.

[11] Ashton S, Song YH, Nolan J, Cadogan E, Murray J, Odedra R, *et al*. Aurora kinase inhibitor nanoparticles target tumors with favorable therapeutic index *in vivo*. Science Translational Medicine. 2016; 8: 325ra17.

[12] Wang C, Chen J, Cao W, Sun L, Sun H, Liu Y. Aurora-B and HDAC synergistically regulate survival and proliferation of lymphoma cell via AKT, mTOR and Notch pathways. European Journal of Pharmacology. 2016; 779: 1–7.

[13] Ambrogio C, Gómez-López G, Falcone M, Vidal A, Nadal E, Crosetto N, *et al*. Combined inhibition of DDR1 and Notch signaling is a therapeutic strategy for KRAS-driven lung adenocarcinoma. Nature Medicine. 2016; 22: 270–277.

[14] Xie C, Wan X, Quan H, Zheng M, Fu L, Li Y, *et al*. Preclinical characterization of anlotinib, a highly potent and selective vascular endothelial growth factor receptor-2 inhibitor. Cancer Science. 2018; 109: 1207–1219.

[15] Beavis PA, Divisekera U, Paget C, Chow MT, John LB, Devaud C, *et al*. Blockade of a2a receptors potently suppresses the metastasis of CD73+ tumors. Proceedings of the National Academy of Sciences of the United States of America. 2013; 110: 14711–14716.

[16] Ruan X, Shi X, Dong Q, Yu Y, Hou X, Song X, *et al*. Antitumor effects of anlotinib in thyroid cancer. Endocrine-Related Cancer. 2019; 26: 153–164.

[17] Han B, Li K, Zhao Y, Li B, Cheng Y, Zhou J, *et al*. Anlotinib as a third-line therapy in patients with refractory advanced non-small-cell lung cancer: a multicentre, randomised phase II trial (ALTER0302). British Journal of Cancer. 2018; 118: 654–661.

[18] He C, Wu T, Hao Y. Anlotinib induces hepatocellular carcinoma apoptosis and inhibits proliferation via Erk and Akt pathway. Biochemical and Biophysical Research Communications. 2018; 503: 3093–3099.

[19] Liang L, Hui K, Hu C, Wen Y, Yang S, Zhu P, *et al*. Autophagy inhibition potentiates the anti-angiogenic property of multikinase inhibitor anlotinib through JAK2/STAT3/VEGFA signaling in non-small cell lung cancer cells. Journal of Experimental & Clinical Cancer Research. 2019; 38: 71.

[20] Wang G, Sun M, Jiang Y, Zhang T, Sun W, Wang H, *et al*. Anlotinib, a novel small molecular tyrosine kinase inhibitor, suppresses growth and metastasis via dual blockade of VEGFR2 and MET in osteosarcoma. International Journal of Cancer. 2019; 145: 979–993.

[21] Ravanan P, Srikumar IF, Talwar P. Autophagy: the spotlight for cellular stress responses. Life Sciences. 2017; 188: 53–67.

[22] Matsuura K, Canfield K, Feng W, Kurokawa M. Metabolic Regulation of Apoptosis in Cancer. International Review of Cell and Molecular Biology. 2016; 327: 43–87.

[23] Sun Y, Du F, Gao M, Ji Q, Li Z, Zhang Y, *et al*. Anlotinib for the Treatment of Patients with Locally Advanced or Metastatic Medullary Thyroid Cancer. Thyroid. 2018; 28: 1455–1461.

[24] Song S, Tan J, Miao Y, Li M, Zhang Q. Crosstalk of autophagy and apoptosis: Involvement of the dual role of autophagy un-

der ER stress. Journal of Cellular Physiology. 2017; 232: 2977–2984.

[25] Heras-Sandoval D, Pérez-Rojas JM, Hernández-Damián J, Pedraza-Chaverri J. The role of PI3K/AKT/mTOR pathway in the modulation of autophagy and the clearance of protein aggregates in neurodegeneration. Cellular Signalling. 2014; 26: 2694–2701.

[26] Zhang W, Hou J, Yan X, Leng J, Li R, Zhang J, *et al*. *Platycodon grandiflorum* Saponins Ameliorate Cisplatin-Induced Acute Nephrotoxicity through the NF-κB-Mediated Inflammation and PI3K/Akt/Apoptosis Signaling Pathways. Nutrients. 2018; 10: 1328.

[27] Yu Y, Lv F, Liang D, Yang Q, Zhang B, Lin H, *et al*. HOTAIR may regulate proliferation, apoptosis, migration and invasion of MCF-7 cells through regulating the P53/Akt/JNK signaling pathway. Biomedicine & Pharmacotherapy. 2017; 90: 555–561.

[28] Zhou Q, Zhou S, Wang H, Li Y, Xiao X, Yang J. Stable silencing of ROR1 regulates cell cycle, apoptosis, and autophagy in a lung adenocarcinoma cell line. International Journal of Clinical and Experimental Pathology. 2020; 13: 1108–1120.